Impurity-site distribution of implanted Bi in iron and nickel studied by channeling and nuclear orientation

P. T. Callaghan,* P. Kittel,† and N. J. Stone
Mullard Cryomagnetic Laboratory, Clarendon Laboratory, Oxford, England

P. D. Johnston
Nuclear Physics Laboratory, Oxford, England
(Received 17 November 1975)

The lattice position occupied by implanted bismuth atoms in iron and nickel single crystals has been studied by observation of Rutherford backscattering from channeled ion beams. In both hosts part of the bismuth distribution was at the surface of the crystal as a result of sputtering during implantation or enhanced diffusion in the heavily damaged region between the surface and the full range depth of the bismuth. Comparison between the bismuth at the full range and the host showed that in neither host did the bismuth occupy a purely substitutional site. In nickel the channeling data are reproduced if 40% of the impurities are associated with dislocation loops oriented in the close-packed (111) planes. In iron the situation is more complicated requiring association with isolated vacancies as well as dislocation loops. Nuclear orientation showed a reproducible hyperfine field for *Ni*Bi but measurements for *Fe*Bi depended on preparation technique. In both hosts a distortion of the host cubic symmetry is required to fit the anisotropies of γ rays deexcitating the 0.128-msec isomer of ^{206}Pb populated in the decay of ^{206}Bi in qualitative agreement with the distortion near dislocation loops required to fit the channeling results.

I. INTRODUCTION

Recent hyperfine-interaction measurements on bismuth atoms implanted in the ferromagnetic lattices of nickel and iron have indicated that the bismuth atoms do not occupy purely substitutional lattice sites in these hosts. The existence of an electric quadrupole interaction in addition to the magnetic dipolar hyperfine interaction, as reported by Johnston and Stone,[1] suggests that the bismuth impurity site does not show the cubic symmetry of the host lattice. This may be either because of a distortion caused by the disparity in ionic sizes of Bi and the hosts, or because the Bi atoms occupy a nonsubstitutional site in the lattice.

Rutherford backscattering from channeled ion beams provides a very sensitive probe to identify and study the location of impurities in single-crystal hosts. In the work discussed here we have used a beam of 3.5-MeV $^{14}N^{+}$ ions to study the distribution of bismuth atoms implanted at a wide range of doses into single crystal hosts of iron and nickel. From the backscattered intensity from the bismuth as a function of the angle between the beam and the crystallographic directions in the major channels we can deduce the symmetry of the impurity sites.

II. COMPUTER SIMULATION OF CHANNELING

To analyze the backscattering data it is necessary to make a comparison between the experimental results of angular scans and the predictions based on a model of the host lattice, the impurity site, and the channeled beam. The model used here is based on the continuum approach developed by Lindhard[2] and used by Alexander, Callaghan, and Poate[3] and by Callaghan.[4] The rows or planes of atoms that bound a channel are considered to be strings or sheets of uniform charge density with the Lindhard potentials[2] within the channels.

An axially channeled ion, parametrized by its transverse energy $E_\perp$, and position r in the transverse plane of the channel, is assumed to have a uniform spatial probability distribution within the accessible area of the channel. The normalized flux at a position r within the channel is then given by numerical integration over all positions of entry for the ion,

$$F(\vec{\mathbf{r}}\psi_i) = \int\int_{A_0} f(\vec{\mathbf{r}}, E_\perp(\psi_i, r_i))r\,dr\,d\theta,$$

where ψ_i is the angle of the incident ion, $\vec{\mathbf{r}}_i$ is the location of the point of entry in the transverse plane, and A_0 is the total area of the channel.

For planar channeling, the spatial probability distribution is assumed to be simple harmonic. This is a good approximation in the center of the channel where the potential can be approximated to that of a simple-harmonic oscillator.

The computed yields for Rutherford backscattering from the host lattice differed in two ways from the experimental results. The calculated minimum yields for substitutional sites were lower than the experimental yields, and the critical angle was smaller. The increased minimum yield observed

experimentally can be attributed to depth effects, not taken into account in the continuum model, radiation damage, and crystal defects, and any oxide layer on the surface. Thus the bismuth yields were renormalized to the experimental minimum yield of the host.

The difference in the critical angles is assumed to result from depth effects and the approximate potentials used. To compensate for this the calculated yields were renormalized in angle ψ_i so that the calculated and experimental host yields have the same angular width.

These corrections were used by Alexander, Callaghan, and Poate[3] and by Callaghan.[4] These authors compared this type of computer simulation to a Monte Carlo simulation based on a binary collision model, and found good agreement between them.

III. CHANNELING IN NICKEL

A. Sample preparation

Implanted nickel single crystals at various impurity doses were studied in these experiments. The implantation was done with the stable isotope of bismuth at 200 keV. Before implantation the nickel crystals were prepared by electropolishing the surface of disks oriented with ⟨111⟩ axis normal to the surface. These disks were spark cut from an oriented single crystal of purity 99.998%.

Several implanted crystals were studied before and after heat treatments. The crystals were sealed under vacuum in quartz ampoules and heated in an oven. After the required heating period the ampoules were allowed to cool slowly. A summary of the bismuth content and heat treatment for each sample is given in Table I.

B. Backscattering spectrum

The channeling was done with 3.5-MeV $^{14}N^{+}$ ions. For each angular scan the dead time of the electronics was kept approximately constant by varying the beam current between 1 and 10 nA. The larger currents were used for counts taken near the center of the channel. The counts were normalized to a net incident charge of 1 μC. The spectra were calibrated in energy using the backscattered edges from unimplanted nickel and bismuth metal.

Spectra from each angular scan were analyzed by summing the counts in two windows, one on the bismuth peak and one on the part of the nickel spectrum corresponding to the same mean depth within the crystal. These sums were plotted as a function of angle. A typical spectrum is shown in Fig. 1.

One of the first things to emerge from the spectrum for the unheated samples with doses of 1×10^{14} and 5×10^{14} atoms/cm^2 was the presence of two bismuth peaks. These peaks, shown in Fig. 2, represent two distributions of bismuth at different depths in the host. The upper peak near the surface of the nickel crystal showed no channeling effect, indicating that in this region the bismuth atoms are randomly distributed with respect to the nickel lattice. The measured fractions of bismuth in this upper peak are summarized in Table II, and are discussed later. A similar surface peak in the bismuth distribution was also seen for the implanted iron crystals, and has also been reported for implanted bismuth in copper.[5] The absence of such a surface concentration in melted dilute alloys suggests that this effect is a result of radiation damage.

TABLE I. Summary of *Ni*Bi and *Fe*Bi implantations.

Host	Bi content dose (ions/cm^2)	Heat treatment (°C for 1 h)	Channeling axes	Nuclear orientation
Ni	1×10^{14}	···	⟨111⟩ ⟨110⟩	
	5×10^{14}	···	⟨111⟩ ⟨110⟩	Yes
		300 °C	⟨111⟩	···
		600 °C	a	Yes
	1×10^{16}	···	a	···
		600 °C	⟨111⟩ ⟨110⟩	···
		700 °C	a	···
Fe	1×10^{14}	···	⟨111⟩ ⟨110⟩	···
	5×10^{14}	···	⟨111⟩ ⟨110⟩ ⟨100⟩	Yes
		600 °C	a	···

[a] Aligned or random measurements along several directions.

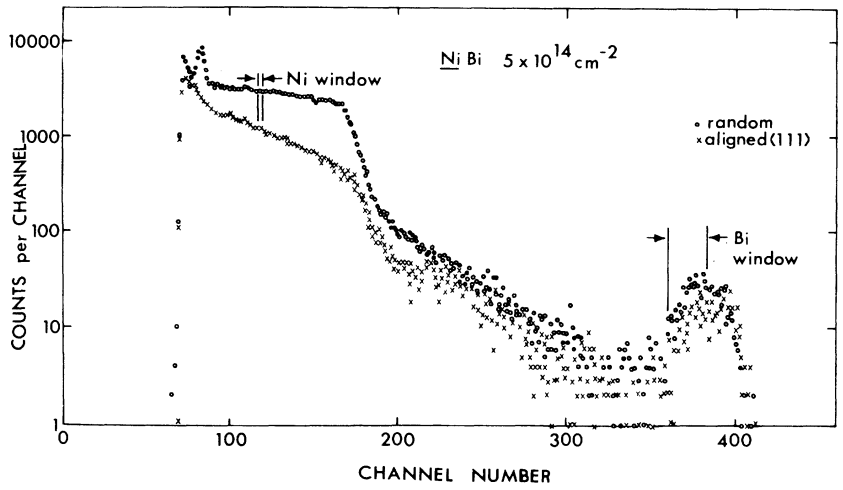

FIG. 1. Backscattered particle-energy spectrum from random and ⟨111⟩ orientations of a nickel single crystal implanted with 5×10^{14} ions/cm^2 of bismuth. Energy windows for the host and full range impurity peak are shown.

C. Surface peak

A review of radiation damage processes has been given by Nelson.[6] There are two principal radiation damage mechanisms in ion implantation. Internal damage occurs when the ion is near the end of its trajectory. In this region the ion loses energy by nuclear collisions that can displace host atoms. From this mechanism the region of maximum damage is expected to be near the region of maximum ion concentration. Such a region can subsequently alter the implanted ion distribution through enhanced diffusion in this region. However, a more direct mechanism for the formation of the surface peak in the depth distribution is provided by sputtering during the implantation. In this process surface atoms are knocked off by incident ions. The number knocked off depends on the type and energy of the incident ion and on the composition of the surface. If the host atoms are preferentially sputtered, the impurities from the sputtered region can remain to form either a surface layer or precipitate. Both a surface layer and precipitates would have only a small hyperfine field and would appear to be randomly distributed to a channeled beam. Heating the crystal may also encourage the formation of precipitates near dislocations. This is especially true when the impurity is very much larger than the host and cannot easily fit into the regular lattice sites. This can be expected for bismuth in nickel since their Goldschmidt radii are 1.82 Å and 1.25 Å, respectively. The presence of precipitates near the surface would account for both the channeling results and the hyperfine interaction measurements by nuclear orientation. (See Sec. IV.)

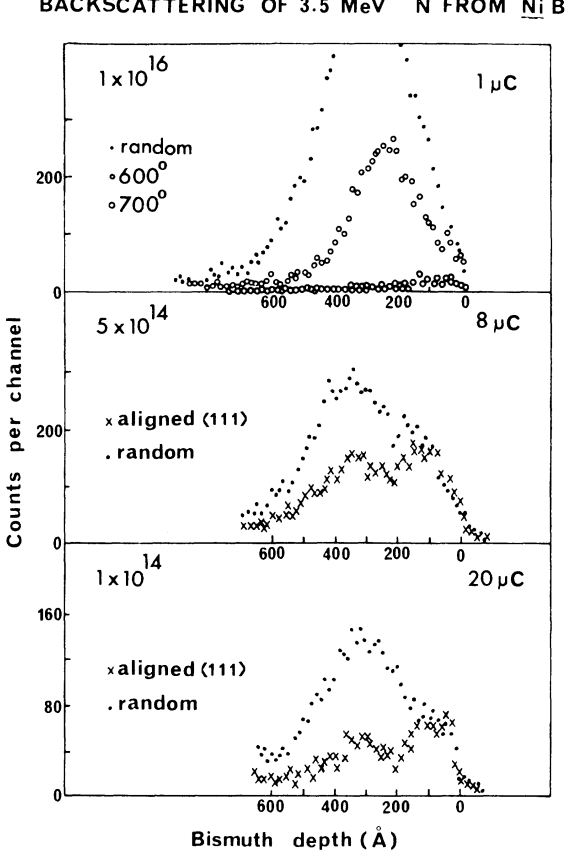

FIG. 2. Backscattered ^{14}N energy spectrum from bismuth implanted in nickel at doses of 1×10^{16}, 5×10^{14} ions/cm^2. Top figure shows the redistribution of the bismuth after annealing at 600° and 700 °C for 1 h. Two lower diagrams show a comparison of the aligned ⟨111⟩ yield and the random yield, with the two bismuth peaks at the surface and the full range depth.

TABLE II. Fraction of implanted bismuth in the surface peak.

Dose (ions/cm^2)	Host	Surface fraction (error) Channeling surface peak (%)	Nuclear orientation (small HFI [a]) (%)
1×10^{14}	Ni	18(3)	...
5×10^{14}	Ni	22(3)	23(3)
5×10^{14} (annealed 600 °C 1 h)	Ni	90(10)	80(5)
5×10^{14}	Fe	12(4)	17(5)

[a] HFI, hyperfine interaction.

D. Full-range peak

All further discussion of the channeling measurements in this section refers to the component in the bismuth distribution at a depth in the nickel corresponding to the full range of the implanted ions in the nickel host. A window can be set on the energy spectrum to exclude the surface peak, and the yield from the bismuth impurities compared as a function of angle with the host lattice.

Results of the scans about the ⟨111⟩ and ⟨110⟩ axes are shown in Fig. 3 for the 5×10^{14} ions/cm^2 sample and in Fig. 4 for the 1×10^{14} ions/cm^2 sample. The important feature of these results is the absence of any prominent structure in the bismuth yields. The minimum yields are intermediate between the values expected for a substitutional site for the impurity, and the absence of any channeling effect for a random site distribution. A linear combination of these two possibilities would, however, give a ratio $[1-\chi_{Bi}(0)]/[1-\chi_{Ni}(0)]$, the same for all channels, where $\chi(\phi)$ is the yield at the angle ϕ from the channel center. This is not the case, as the ratio of minimum yields is ~0.5 for the ⟨110⟩ axis and 0.75 for the ⟨111⟩ axis scan.

The observed angular scans are also inconsistent with a unique interstitial site of high symmetry for the bismuth. The effect of flux peaking, described by Alexander,[7] gives pronounced structure to the angular scans because of the enhanced backscattered yield from any specific impurity sites within the channel. No such structure is observed and thus it is unlikely that any such specific site can be supported.

Because of the disparity in the ionic sizes of the bismuth and nickel host it is useful to consider the regions of lattice distortion associated with defects. Some information exists for the system of XeFe studied by De Waard.[8] Drentje and Ekster[9] have developed a theory to explain the hyperfine interaction measurements of the xenon impurity involving the interaction with single vacancies in the lattice. Hyperfine-field measurements are consistent with impurity atoms displaced by the influence of isolated neighboring vacancies. Com-

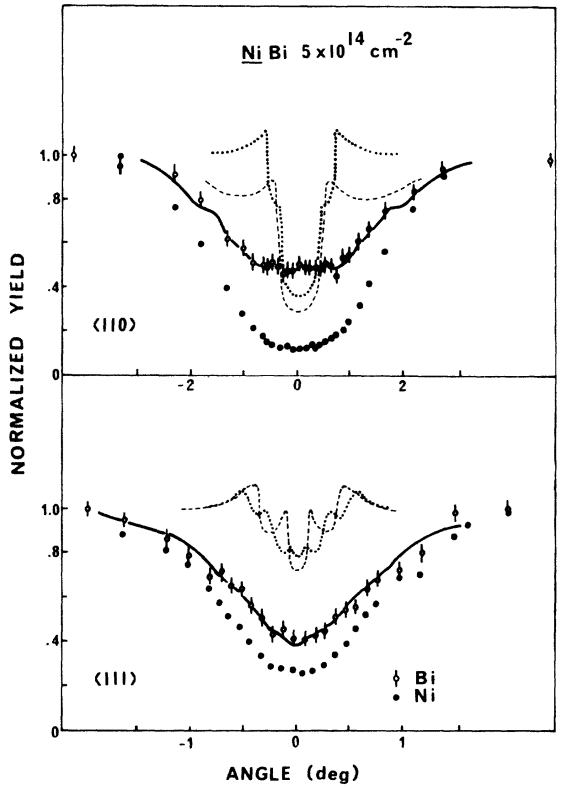

FIG. 3. Angular scans across the ⟨110⟩ and ⟨111⟩ axes of the nickel host. Implantation dose is 5×10^{14} ions/cm^2. Dotted line shows the calculated yield for impurities shifted by $\frac{1}{5}$ of the interatomic distance towards a nearest-neighbor vacancy. Dashed line is for a similar shift of $\frac{1}{4}$ of the interatomic distance. Solid line is the calculated yield with 60% undistorted substitutional and 40% displaced primarily along the ⟨111⟩ directions to simulate the effect of association with dislocation loops.

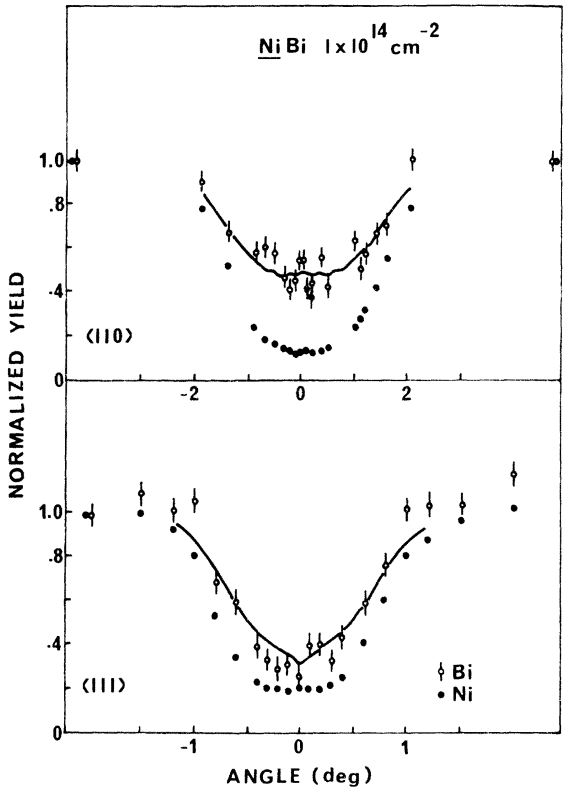

FIG. 4. Angular scans for the ⟨110⟩ and ⟨111⟩ axes at an implantation dose of 1×10^{14} ions/cm^2. Solid line is the calculated yield for 60% substitutional and 40% displaced primarily along the ⟨111⟩ directions.

puter calculations of the lattice relaxation suggest a displacement of the impurity towards a nearest-neighbor vacancy of $\frac{1}{4}$ of the nearest-neighbor distance. Callaghan *et al.*[10] found that this single vacancy model is also consistent with observations in the *Fe*I system.

In the fcc nickel lattice the nearest neighbors lie in the ⟨100⟩ directions. In Fig. 3 the yields calculated for a displacement of $\frac{1}{4}$ and $\frac{1}{5}$ of the nearest-neighbor distance are shown. They show that this single vacancy model does not explain the observations of the *Ni*Bi system.

Single vacancies are not the only form of crystal damage present in implanted crystals. Large numbers of dislocation loops are also present. These loops are clusters of interstitials or vacancies. The properties of these loops have been reviewed by Thompson[11] and by Maher and Eyre.[12] Calculations show that they have a lower energy than single interstitials or vacancies, and form preferentially in the close-packed planes. These are the (111) planes in an fcc lattice. It has been confirmed that dislocation loops lie in (111) planes by Mazey and Hudson[13] for proton irradiated nickel and by Harbottle[14] for neutron irradiated nickel. The size and number of these loops increases with dose.

In the vicinity of these loops the lattice is distorted. This distortion is characterized by a Burgers vector, which represents the displacement of the atoms immediately surrounding the loop from their position in an ideal lattice. For a loop in a (111) plane the Burgers vector is in the ⟨111⟩ direction. This distorted region would provide an ideal site for the large bismuth atoms. Even when the initial position of an implanted ion is substitutional, it remains free to move to more favorable sites by vacancy exchange at room temperature.[6]

Using a computer-simulation technique, Morgan and Van Vliet[15] found that a substitutional atom in the distorted region will not appear to be substitutional to a channeled beam. It will appear to be displaced into the channel. The displacement is principally in the direction of the Burgers vector. Atoms near the edge of the loop, the region of maximum distortion, will also have a displacement component perpendicular to the Burgers vector.

We have attempted, in the light of these considerations, to reproduce the experimental angular yields using the following model. A proportion of the bismuth atoms are assumed to be substitutional, in sites sufficiently far from lattice defects to be seen as unshifted by the channeled beam. The remaining atoms are considered as substitutional or only slightly displaced from a substitutional site, but in the distorted region of the lattice associated with dislocation loops. These sites are seen as displaced principally along a ⟨111⟩ axis, but also with a much smaller distribution of displacements in the plane normal to this axis.

Computer simulations of the angular yields were made on the assumption that this latter proportion are distributed uniformly along the ⟨111⟩ axes, and have a Gaussian distribution of displacements in the (111) planes, with a characteristic displacement a.

Using this model it was possible to reproduce the angular scans along all the measured axes with 60% pure substitutional and 40% near dislocation loops. The characteristic displacement transverse to the Burgers vector was 0.35 Å. This distance is small compared with the nearest-neighbor distance of 2.49 Å. The calculated yields are not very sensitive to the exact form of the displacement distributions, but agreement with experiment does require displacements predominantly along the ⟨111⟩ axes.

E. Annealing effects in *Ni*Bi

The most significant effects of annealing at all implantation doses were the migration of bismuth

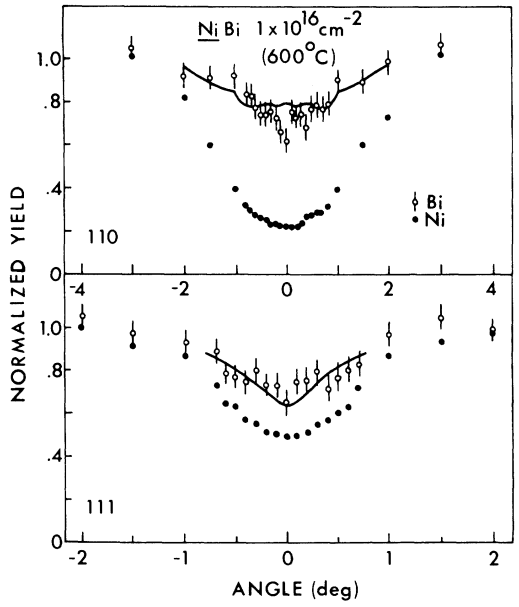

FIG. 5. Angular scans for the ⟨110⟩ and ⟨111⟩ axes for the implanted dose of 1×10^{16} ions/cm^2 after annealing for 1 h at 600 °C. Solid line is the calculated yield for 25% substitutional and 75% displaced primarily along the ⟨111⟩ directions.

to the surface of the crystals, and loss by evaporation. For the dose of 5×10^{14} cm^{-2}, an hour at 300 °C reduced the amount of bismuth in the lower energy (greater depth) peak of the backscattered spectrum to 25% of the unannealed value. After 1 h at 600 °C only the surface peak remained.

Crystals were also prepared at much greater implantation doses up to 1×10^{16} cm^{-2}. The unannealed samples showed no channeling effect on bismuth, indicating that the bismuth atoms were distributed randomly. This was probably due to the large amount of damage caused at this high dose. Heating the crystal again resulted in migration of bismuth to the surface with losses due to evaporation. Annealing also removes some crystal damage by increasing the mobility of the vacancies and dislocation loops.[6,12] After annealing at 600 °C for 1 h the bismuth backscattering peak showed some channeling effect. These measurements are shown in Fig. 5 with the calculated yields for 25% pure substitutional and 75% displaced along ⟨111⟩ axes. The agreement is not as good as for lower dose samples; however, with a large degree of damage some dislocation loops may no longer lie in the (111) planes. Large loops rotate out of the close-packed planes by shearing. When this happens in fcc crystals, Bullough and Foreman[16] have shown that the Burgers vector will change from the ⟨111⟩ direction to the ⟨110⟩ direction. This has been observed in aluminum crystals

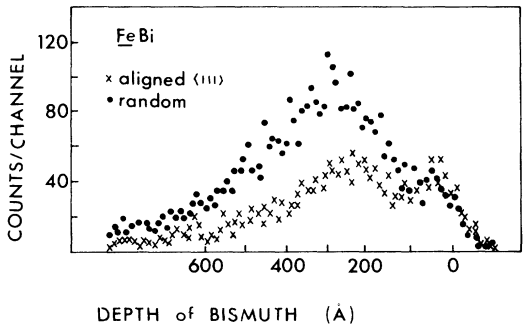

FIG. 6. Backscattered ^{14}N energy spectrum from bismuth implanted in an iron single crystal at a dose of 5×10^{14} ions/cm^2. Random orientation and aligned ⟨100⟩ orientation are shown.

by Makin and Hudson[17] and by Strudel and Washburn.[18] The disagreement between the calculated yields and the data for the high dose may be a result of some of the Burgers vectors changing orientation, with some bismuth displaced along the ⟨110⟩ axes.

A similar association of bismuth impurities with lattice defects may be expected in thermally prepared alloys if the temperature of preparation is sufficiently high to excite a significant population of vacancy-interstitial pairs. The hyperfine interaction measurements in implanted and diffused *Ni*Bi alloys discussed in Sec. V suggest a similar site distribution for both preparation techniques.

IV. CHANNELING IN *Fe*Bi

A. Sample preparation

The iron crystal surfaces were prepared by electropolishing and were implanted with bismuth doses of 1×10^{14} and 5×10^{14} cm^{-2}. The ⟨111⟩ and ⟨110⟩ axial channels were scanned with the implantation dose of 1×10^{14} cm^{-2}, and the ⟨111⟩, ⟨110⟩, and ⟨100⟩ channels with the 5×10^{14} dose. The experimental procedure was identical to that for the nickel crystals.

B. Surface peak

A surface peak was again seen in the backscattered spectrum. The peak was smaller and less easily resolved than in the nickel experiments, being only fully resolved on the ⟨100⟩ scan of the 5×10^{14} dose. (See Fig. 6.) On this scan the beam was incident at 45° to the surface normal. Because the implanted ions lie in a narrow layer the depth resolution in this layer is improved by a factor of 2. The surface peak contained 12(4)% of the implanted bismuth, which, as shown in Table II, is in reasonable agreement with the 17(5)%

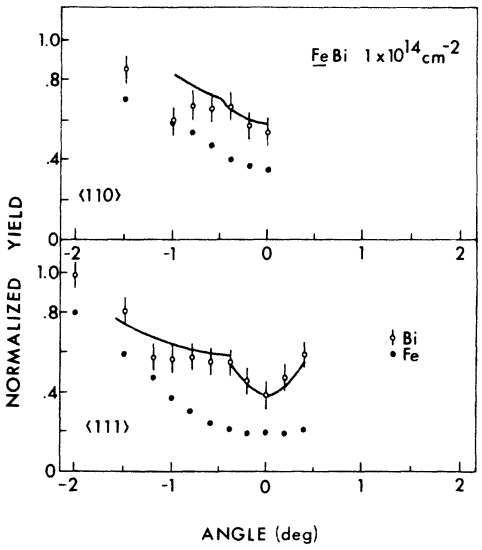

FIG. 7. Angular scans for the ⟨110⟩ and ⟨111⟩ axes of iron, with an implanted bismuth dose of 1×10^{14} ions/cm^2. Solid line is the calculated bismuth yield for a distribution of sites including 40% substitutional, 30% shifted by $\frac{1}{4}$ of the interatomic distance towards a nearest neighbor, and 30% displaced along the ⟨110⟩ directions.

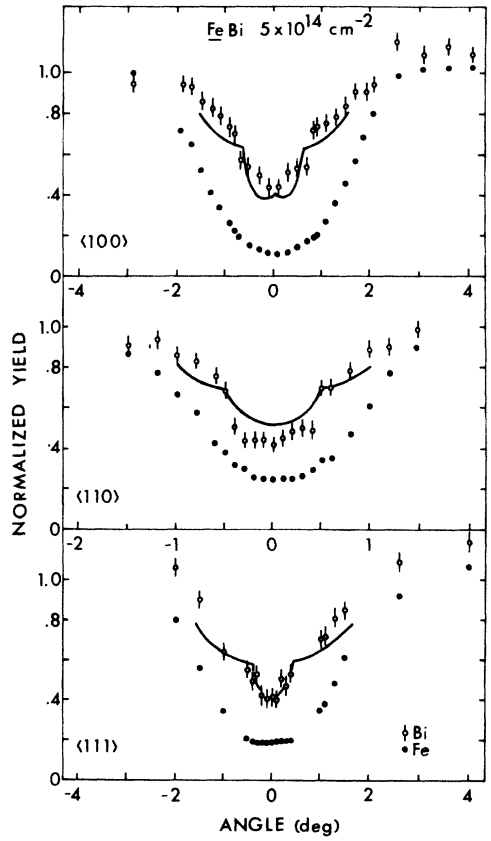

FIG. 8. Angular scans across the ⟨100⟩, ⟨110⟩, and ⟨111⟩ axes of iron with an implanted bismuth dose of 5×10^{14} ions/cm^2. Solid line is the calculated bismuth yield for the site distribution: 40% substitutional; 30% shifted by $\frac{1}{4}$ of the interatomic distance towards a nearest-neighbor vacancy; 30% displaced along ⟨110⟩ directions.

found in the orientation experiments for the proportion of bismuth in low-field sites. The smaller surface peak in iron compared with nickel is consistent with experimental findings of Almen and Bruce.[19] These authors studied the sputtering of Fe, Ni, and Bi by Cu, Kr, Ag, and Ta beams. In all cases they found iron was less susceptible to sputtering than nickel.

C. Angular scans on the full range peak

Data from the angular scans on the full range component in the bismuth distribution are shown in Figs. 7 and 8 for the same doses and axes as *Ni*Bi.

In the bcc structure of iron the close-packed planes are the (110) planes. However, the orientation of dislocation loops is not well established. Eyre and Bullough[20] predicted that the Burgers vectors of large dislocation loops would rotate to the [111] and [100] directions. Dingley and Hale[21] have seen all three orientations of Burgers vectors in strain deformed iron. Eyre and Bartlett[22] have seen ⟨111⟩ Burgers vectors in neutron irradiated iron, while Masters[23] has seen ⟨100⟩ Burgers vectors in iron implanted iron. Bullough and Perrin[24] have suggested that the Burgers vector will change to the ⟨111⟩ direction in low-temperature implantations and to the ⟨100⟩ direction at high temperatures.

We have found, however, that the channeling data on bismuth in iron are not consistent with any combination of large displacements along these three principle directions. A combination of the single vacancy model[8] with substitutional and dislocation loop sites was then tried. By including a proportion of nearest-neighbor vacancies our computer simulations give good agreement with the channeling data with 40% of the bismuth pure substitutional, 30% displaced from the substitutional site by a nearest-neighbor vacancy, and 30% randomly distributed along ⟨110⟩ axes. A displacement of $\frac{1}{4}$ of the nearest-neighbor distance was used in the calculation of the channeling yields for the proportion of bismuth impurities with nearest-neighbor vacancies.[9]

Agreement with the experimental data was best with a proportion of the bismuth randomly distributed along the ⟨110⟩ cases, but additional displacements along ⟨100⟩ and ⟨111⟩ directions were also possible within the experimental uncertainty.

The experimental uncertainty did not allow any

effects of next-nearest-neighbor or more remote vacancies to be observed.

V. HYPERFINE-INTERACTION MEASUREMENTS

A. Introduction

Implanted bismuth in nickel and iron crystals was also studied by low-temperature nuclear orientation. The dose of 5×10^{14} cm^{-2} containing 20 μCi of ^{206}Bi was the same as in the principal channeling measurements. The implantation energy was 80 keV. The hyperfine interaction information obtained from the nuclear orientation measurements is important in allowing the site distribution from the channeling measurements to be correlated with the distribution of magnetic dipole and electric quadrupole hyperfine interactions.

B. Orientation in nickel

The mean magnetic hyperfine field at bismuth in nickel, prepared by thermal alloying is known from previous work.[25] Bismuth is soluble in nickel, and the reproducibility of the hyperfine interaction measurements on thermally prepared alloys suggests that in such alloys the bismuth occupies a typical site or distribution of sites with a well-defined mean hyperfine interaction. The γ-ray distributions from the implanted bismuth oriented at temperatures between 50 and 15 mK showed smaller anisotropies than those from the thermally prepared alloys. However, a good fit to the data from the implanted material was obtained consistent with 77(3)% of the bismuth experiencing the same average hyperfine interaction as measured in the thermally prepared alloys [390(15) kOe], and the remaining 23(3)% experiencing only a very small or zero magnetic interaction. In Table II it can be seen that this proportion corresponds to the amount of bismuth observed in the surface peak of the backscattered ^{14}N spectrum.

After heating to 600 °C for 1 h the fraction of bismuth with little or no hyperfine interaction increased to 80(5)%, again corresponding to the migration to the surface observed in the channeling experiment.

Attempts to observe nuclear magnetic resonance on the oriented bismuth nuclei failed in both implanted and thermally prepared alloys, although the observed γ-ray anisotropies were large. This suggests a wider distribution in magnetic resonance frequencies than is usually associated with the inhomogeneity effects for substitutional impurities. A wider variation for *Ni*Bi can be associated with electric quadrupole interactions or small differences in the magnetic hyperfine interaction between the purely substitutional site and the sites near dislocation loops. The anisotropy measurement is not sensitive to such distributions (±10%) in the hyperfine interaction and can only confirm the separation of the implanted Bi between high- and low-field sites in the Ni host.

A feature of the nuclear orientation measurements on thermally prepared alloys of bismuth in nickel and iron, reported by Johnston and Stone,[1] is the reorientation in the metastable states of Pb populated in the decay. This effect can be attributed to the existence of an electric field gradient at the bismuth site associated with a local distortion of the cubic symmetry of the host. Reorientation in the 2.2-MeV excited state of ^{206}Pb, of lifetime 0.128 msec, was again present in the implanted alloys. The evidence of the channeling measurements indicates that a proportion of the bismuth impurities are associated in nickel and iron with dislocation loops. It is just such impurity sites in distorted regions of the crystal lattice that experience electric quadrupole interactions. It is not possible in an integral measurement such as nuclear orientation provides, to measure the distribution of such quadrupole interactions, since only an average over all nuclei seeing the large magnetic interaction is measured.

The temperature dependence of the anisotropies of γ rays following population of the 2.2-MeV state fitted the calculated values for a ratio of the electric quadrupole to magnetic dipole hyperfine interaction strength[1] of 0.11 ± 0.02 compared with the value 0.112 ± 0.005 in thermal alloys. This agreement is further confirmation that the implanted Bi atoms have the same site distribution as in the thermal *Ni*Bi alloys.

C. Orientation in iron

An unannealed alloy of implanted Bi in Fe showed larger γ-ray anisotropies than observed for any thermally prepared source; however, thermal alloys had to be quenched very rapidly from 1600 °C to keep the Bi atoms in sites showing appreciable hyperfine interaction. This is associated with the very low solubility of Bi in Fe at room temperature. The proportion of Bi atoms "frozen" into sites with a large magnetic hyperfine interaction depends on the rate of cooling.

The orientation results from implanted ^{206}Bi in Fe were analyzed by fitting with two independent parameters; the magnetic hyperfine field and the fraction of Bi nuclei experiencing very small or zero field. The best fit was obtained for 83(5)% of the implanted Bi experiencing a field of 1370(50) kOe and 17(5)% in low-field sites. The latter figure compared well with the 12(4)% found in the surface peak in Fe implants. The value of the

field is greater than the values obtained by Bacon *et al.*,[26] 1180(13) kOe, and Kaplan *et al.*,[25] 900(100) kOe using melted and quenched alloys. As in the Ni hosts we were unable to observe resonance of the Bi nuclei. This difficulty and the variation of results with preparation techniques reflects the low solubility of Bi in iron and may also be related to the affinity of bismuth for lattice defects in iron shown by the channeling measurements.

In the iron host the attenuation of the anisotropy of the γ transitions on de-excitation of the 2.2-MeV excited state of ^{206}Pb was markedly greater than for the thermally prepared alloys, being fitted by the $E2/M1$ ratio $x = 0.09 \pm 0.01$. The best fit in thermal alloys was $x = 0.05 \pm 0.01$. Thus both the magnitude of the magnetic interaction and the perturbation of the 0.128-msec isomer of ^{206}Pb indicate different site distributions for Bi in implanted and quenched iron alloys. A comparison of orientation results from quenched and implanted *Fe*Bi alloys is shown in Fig. 9.

On the basis of measurements of larger hyperfine fields in annealed alloys than implanted bismuth, Feldman *et al.*[27] suggested that a larger field should be associated with nonsubstitutional sites. Our measurements show that the annealing of implanted samples reduces the substitutional fraction and net hyperfine field because of migration to the surface layer. There are differences between the bismuth fields in implanted and quenched alloys, but in the light of the ready association of the bismuth impurities with crystal defects, the different defect structures produced in these two preparation techniques will affect the hyperfine field. Our results show that the large hyperfine field should be associated with the substitutional and distorted substitutional lattice sites, not with the randomly distributed bismuth in a surface layer.

VI. CONCLUSIONS

The angular scans across the major channeling axes of nickel and iron hosts containing a dilute impurity of implanted bismuth show a distribution for the bismuth sites, different from that of the host atoms. In both hosts fractions of the bismuth distribution are observed at different depths. A surface layer, randomly distributed to the channeling beam, is identified with the proportion of the implanted bismuth experiencing very little hyperfine interaction. Our measurements show that the onset of the marked reduction in the total substitutional fraction of bismuth observed by Feldman *et al.*[27] at 600 °C is associated with implanted bismuth in the region of heavy radiation

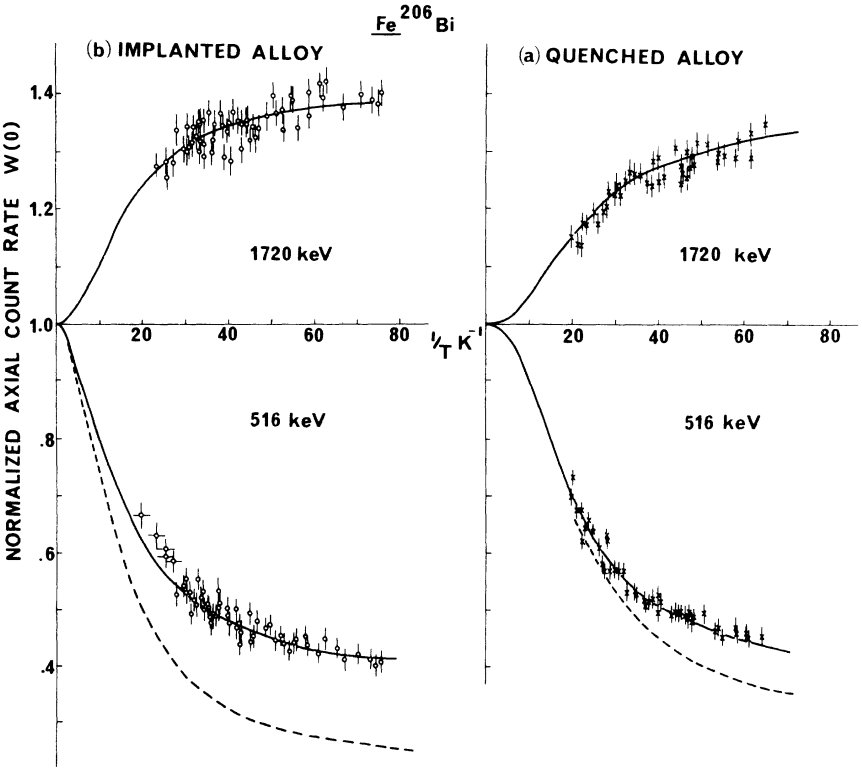

FIG. 9. Normalized axial counting rate as a function of temperature for the 1720- and 516-keV γ rays in the decay of ^{206}Bi oriented in iron. (a) Shows results from a quenched alloy; the solid line is the calculated temperature dependence for a field of 900 kOe. 516-keV γ ray anisotropy is attenuated by electric quadrupole interactions in the 2.2-MeV excited state of ^{206}Pb. (b) Shows the results from the implanted *Fe*Bi alloy. Solid line is for a field of 1370 kOe.

damage migrating to the surface.

The distribution of bismuth in nickel at the depth corresponding to the full range of the implanted ions shows a structure in the channeling measurements in good agreement with the computed yields for 60% purely substitutional and 40% displaced from the regular sites by the lattice distortion associated with dislocation loops in the close-packed planes. The existence of a nonzero electric quadrupole contribution in the hyperfine interaction is consistent with the channeling picture of a proportion of impurity atoms in a distorted region of the host lattice.

The channeling in iron shows a more complicated site distribution, with a possible explanation including single vacancy interactions in addition to dislocation loop distortion.

In contrast with the conclusions of Feldman *et al.* our measurements show that the large hyperfine interaction of bismuth in iron should be associated with substitutional sites. A distinction must be made between implanted alloys annealed at >600 °C and melted alloys quenched from 1500 °C. For the implanted material the substitutional fraction and net hyperfine interaction both drop rapidly for annealing temperature >600 °C because of the migration of bismuth to the surface layer. The hyperfine interaction in rapidly melted or quenched alloys is broadly similar to that of unannealed implanted alloys. The differences in iron may be attributed to the different vacancy and damage structures for these two preparation techniques, accentuated by the extremely low solubility of bismuth in iron.

ACKNOWLEDGMENTS

This work has been made possible by grants from the Science Research Council and a Research Fellowship (P.D.J.) all of which are gratefully acknowledged. The authors would like to thank G. Read for preparing the crystals and W. Temple for performing the implantations.

---

*Present address: Dept. of Biophysics, Massey University, Palmeston North, New Zealand.

†Present address: Dept. of Physics, University of Oregon, Eugene, Ore..

[1]P. D. Johnston and N. J. Stone, J. Phys. F 4, 1522 (1974).

[2]J. Lindhard, Dan Vidensk. Selsk. Mat.-Fys. Medd. 14, 34 (1965).

[3]R. B. Alexander, P. T. Callaghan, and J. M. Poate, Phys. Rev. B 9, 3022 (1974).

[4]P. T. Callaghan, Phil. thesis (Oxford University, 1973) (unpublished).

[5]H. H. Anderson, Radiat. Eff. 19, 257 (1973).

[6]R. S. Nelson, *Defects in Crystalline Solids*, edited by S. Amelinckx, R. G. Gevers, and J. Nihoul (North-Holland, Amsterdam, 1973), Vol. 8, p. 154.

[7]R. B. Alexander, Ph.D. thesis (Oxford University, 1971) (U.K.A.E.R.E.-Report No. 6849) (unpublished).

[8]H. De Waard, R. L. Cohen, S. R. Reintsema, and S. A. Drentje, Phys. Rev. B 10, 3760 (1974).

[9]S. A. Drentje and J. Ekster, J. Appl. Phys. 45, 3242 (1974).

[10]P. T. Callaghan, P. K. James, and N. J. Stone, Phys. Rev. B 12, 3553 (1975).

[11]M. W. Thompson, *Defects and Radiation Damage in Metals* (Cambridge U. P., London, 1969).

[12]D. M. Maher and B. L. Eyre, Philos. Mag. 23, 409 (1971).

[13]P. J. Mazey and J. A. Hudson, J. Nucl. Mater. 37, 13 (1970).

[14]J. E. Harbottle, Philos. Mag. 27, 147 (1973).

[15]D. V. Morgan and D. Van Vliet, Proceedings of the Conference on Atomic Collisions and Phenomena, Sussex, 1974 (unpublished), p. 476.

[16]R. Bullough and A. J. E. Foreman, Philos. Mag. 9, 315 (1964).

[17]M. J. Makin and B. Hudson, Philos. Mag. 8, 447 (1963).

[18]J. L. Strudel and J. Washburn, Philos. Mag. 9, 491 (1964).

[19]O. Almen and G. Bruce, Nucl. Instrum. Methods 11, 257 (1961); 11, 279 (1961).

[20]B. L. Eyre and R. Bullough, Philos. Mag. 12, 31 (1965).

[21]D. J. Dingley and K. F. Hale, Proc. R. Soc. A 292, 55 (1966).

[22]B. L. Eyre and A. F. Bartlett, Philos. Mag. 12, 261 (1965).

[23]B. C. Masters, Central Electricity Generating Board Reports No. RD/B/N245 and No. RD/B/N321 (unpublished).

[24]R. Bullough and R. C. Perrin, Proc. R. Soc. A 305, 541 (1968).

[25]M. Kaplan, P. D. Johnston, P. Kittel, and N. J. Stone, Phys. Lett. A 41, 315 (1972).

[26]F. Bacon, H. Hass, G. Kaindl, and H. E. Mahnke, Phys. Lett. A 38, 401 (1972).

[27]L. C. Feldman, E. N. Kaufmann, D. W. Mingay, and W. M. Augustyniak, Phys. Rev. Lett. 27, 1145 (1971).